

Immune synapse formation determines interaction forces between T cells and antigen-presenting cells measured by atomic force microscopy

Babak H. Hosseini^a, Ilia Louban^a, Dominik Djandji^b, Guido H. Wabnitz^c, Janosch Deeg^a, Nadja Bulbuc^b, Yvonne Samstag^c, Matthias Gunzer^d, Joachim P. Spatz^a, and Günter J. Hammerling^{b,1}

^aDepartment of New Materials and Biosystems, Max-Planck-Institute for Metals Research, Stuttgart, Germany, and Department of Biophysical Chemistry, University of Heidelberg, Heisenbergstrasse 3, D-70569 Stuttgart, Germany; ^bDepartment of Molecular Immunology, German Cancer Research Center, D-69120 Heidelberg, Germany; ^cInstitute for Immunology, University of Heidelberg, Im Neuenheimer Feld 305, D-69120 Heidelberg, Germany; and ^dInstitute of Molecular and Clinical Immunology, Otto-von-Guericke-University-Magdeburg, Leipziger-Strasse 44, D-39120 Magdeburg, Germany

Edited by Michael Sela, Weizmann Institute of Science, Rehovot, Israel, and approved September 3, 2009 (received for review May 19, 2009)

During adaptive immune responses, T lymphocytes recognize antigenic peptides presented by MHC molecules on antigen-presenting cells (APCs). This recognition results in the formation of a so-called immune synapse (IS) at the T-cell/APC interface, which is crucial for T-cell activation. The molecular composition of the IS has been extensively studied, but little is known about the biophysics and interaction forces between T cells and APCs. Here, we report the measurement of interaction forces between T cells and APCs employing atomic force microscopy (AFM). For these investigations, specific T cells were selected that recognize an antigenic peptide presented by MHC-class II molecules on APCs. Dynamic analysis of T-cell/APC interaction by AFM revealed that in the presence of antigen interaction forces increased from 1 to 2 nN at early time-points to a maximum of ≈ 14 nN after 30 min and decreased again after 60 min. These data correlate with the kinetics of synapse formation that also reached a maximum after 30 min, as determined by high-throughput multispectral imaging flow cytometry. Because the integrin lymphocyte function antigen-1 (LFA-1) and its counterpart intercellular adhesion molecule-1 (ICAM-1) are prominent members of a mature IS, the effect of a small molecular inhibitor for LFA-1, BIRT377, was investigated. BIRT377 almost completely abolishes the interaction forces, emphasizing the importance of LFA-1/ICAM-1-interactions for firm T-cell/APC adhesion. In conclusion, using biophysical measurements, this study provides precise values for the interaction forces between T cells and APCs and demonstrates that these forces develop over time and are highest when synapse formation is maximal.

Cell-cell contacts play a crucial role in triggering the body's immune system. During adaptive immune responses, antigen-presenting cells (APCs) process foreign antigens into peptides, which are loaded into major histocompatibility complex (MHC) molecules. T cells patrolling the body scan APC and establish intercellular contacts when their antigen-specific T-cell receptors (TCR) recognize a foreign peptide/MHC complex on the APC. Elegant two-photon microscopy studies have revealed the dynamics of this process in lymph nodes. There, T cells move through the network of dendritic cells (DCs) and scan DCs for foreign antigen. In the absence of antigen brief transient interactions are observed, whereas upon recognition of a cognate antigen T cells are arrested and interactions prolonged to >1 h (1, 2). Similarly, during antibody responses, long-lasting antigen driven interactions between T helper cells and B cells have been observed in lymph nodes (3). Subsequently, at the contact zone between T cells and APC spatially organized molecular clusters develop, referred to as immune synapse (IS), which is crucial for T-cell activation and effector cells development (4).

Formation of an IS includes the coordinated translocation of several protein complexes, among others TCR and its ligand pMHC, and the integrin lymphocyte function-associated antigen-1 (LFA-1) and its counterpart intercellular adhesion mole-

cule 1 (ICAM-1). This orchestrated reorganization of membrane proteins involves many cytoplasmic molecules and is presumably supported by cytoskeletal factors like actin (5). Although many important aspects of IS formation have been identified, little is known about the underlying biophysics and interaction forces between T cells and APCs. Integrins represent a family of major cell adhesion proteins used by cells to tune their adhesion propensity. This tuning is achieved by controlling the number of proteins present at the cell's interaction face and by the activation state of the adhesion proteins themselves. Switch blade-type heterodimeric integrins are known to exist in different activation states, which are transmitted from the cytoplasmic tail to the extracellular domain (6). It is believed that activation state changes are triggered by inside-out-signaling, for instance when a TCR recognizes a peptide presented by MHC molecules (7). The activation of LFA-1 upon TCR-triggering is mainly mediated by PKC and the small GTPases Ras and Rap1 [(8) and references therein]. The association of actin to LFA-1 accompanies this process. Subsequent motor protein motion yields a cytoskeleton contraction, which exerts low forces on LFA-1 to induce occupied integrin activation and to fully arrest the two cells for adhesion. By *actio et reactio*, this force has to be counterbalanced on the APC side, resulting in a high interaction force between T cells and APCs.

Cell-cell adhesion has been studied by micropipette aspiration techniques (9, 10) and atomic force microscopy (AFM) (11–13). The recent years have seen a significant increase of AFM-related studies in biological systems, and single-cell force spectroscopy (SCFS) by AFM has been established as an important tool for the study of cell adhesion (14). This technique allows for the analysis of adhesion processes and adhesion forces under near-physiological conditions. To the best of our knowledge, the interaction forces between T cells and APC have not yet been investigated by SCFS. In the present study, we have modified and adjusted SCFS techniques for the measurement of long-time interaction forces between T cells and APC. These force spectroscopy measurements were complemented by conjugate and high-throughput fluorescence assays relating the kinetics of IS formation to the development of interaction forces between T cells and APCs.

Results

Conjugate Formation Between T Cells and APCs. For the present work, a well-studied T-cell/APC pair was selected, namely the

Author contributions: B.H.H., I.L., D.D., Y.S., M.G., J.P.S., and G.J.H. designed research; B.H.H., D.D., G.H.W., J.D., and N.B. performed research; B.H.H., I.L., G.H.W., and G.J.H. analyzed data; and B.H.H. and G.J.H. wrote the paper.

The authors declare no conflict of interest.

This article is a PNAS Direct Submission.

¹To whom correspondence should be addressed. E-mail: hammerling@dkfz.de.

This article contains supporting information online at www.pnas.org/cgi/content/full/0905384106/DCSupplemental.

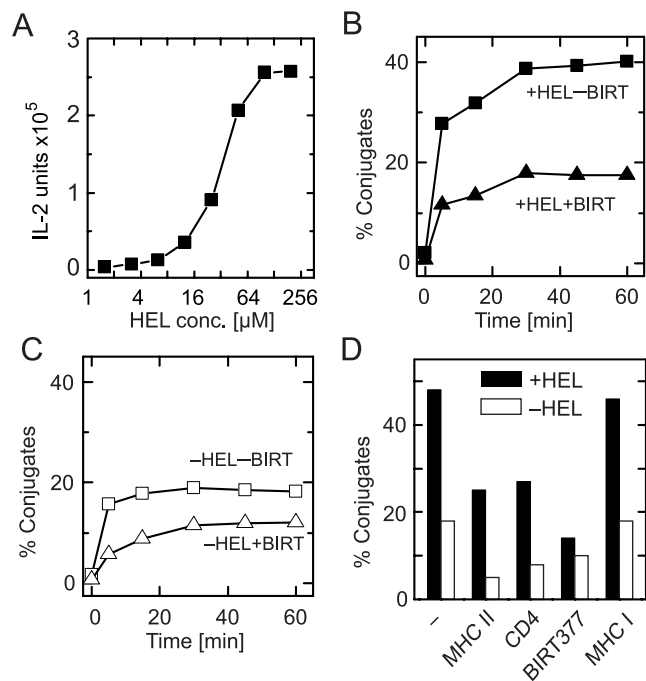


Fig. 1. Antigen presentation and conjugate formation between T cells and APCs. (A) Presentation of HEL_{34–45} by Lk35.2 APCs to 3B11 T cells results in IL-2 secretion. (B and C) Kinetics of conjugate formation between 3B11 T cells and LK35.2 APCs in the presence (B) and absence (C) of HEL_{34–45} peptide, and inhibition with 80 μM LFA-1 antagonist BIRT377 (triangles). (D) Inhibition of conjugate formation by antibodies against MHC-II, CD4, MHC-I, and BIRT377. Conjugates were allowed to form for 30 min in the presence (black bars) or absence (white bars) of HEL_{34–45} peptide. For inhibition, 10 μg/mL antibody were used. For detailed inhibition curves, see Fig. S2.

3B11 T hybridoma and the LK35.2 B cell line (15), because in orientating experiments 3B11 cells could be attached well via antibodies to the cantilever of the AFM instrument. The 3B11 T hybridoma recognizes a peptide HEL_{35–45} derived from the model antigen hen egg lysozyme presented by Ak MHC class II-positive APC, such as LK35.2 B cells. Fig. 1A shows that LK35.2 cells loaded with HEL_{35–45} peptide stimulated IL-2-production by 3B11 T cells, whereas irrelevant peptide failed to stimulate 3B11 (data not shown). Because IL-2-secretion was highest at 100 μmol peptide concentration, for further studies this concentration was used. Fig. S1 shows the expression of surface markers such as Ak, ICAM-1, LFA-1, CD3, and CD43, which are relevant for the present study.

Next, we analyzed whether 3B11 T cells and LK35.2 APCs would adhere to each other in the presence of peptide and form conjugates. For this purpose, 3B11 cells were labeled with the green dye CFSE and LK35.2 with the red dye SNARF (16). Cells were mixed at a 1:1 ratio, centrifuged briefly, and incubated for various times before fixation with paraformaldehyde. Conjugates were identified by FACS analysis by virtue of simultaneous green and red signals. Fig. 1B shows that within the first 5 min, the majority of contacts are formed in the presence of peptide, ≈28% in this particular experiment. The cell adhesion molecules ICAM-1 and LFA-1 have been reported to play a role in the interaction between T cells and APCs (16). Therefore, we analyzed whether the small molecule antagonist BIRT377, which inhibits the high-affinity state of LFA-1, would interfere with conjugate formation (17). Fig. 1B shows that BIRT377 blocked conjugate formation effectively, thus demonstrating the importance of LFA-1/ICAM-1 interactions in this process.

Conjugates formed also in the absence of peptide, albeit to a lower degree (Fig. 1C). These spontaneous conjugates were also

blocked by BIRT377. To see whether additional cell surface molecules would contribute to conjugate formation, we included antibodies against MHC and CD4 molecules. Antibodies against CD4 and MHC class II molecules inhibited conjugate formation, but not anti-MHC class I antibody (Fig. 1D). These results were expected for the peptide-dependent conjugate, because the TCR of 3B11 T cells recognizes peptide MHC class II complexes in a CD4-dependent fashion. The same inhibition pattern was observed for spontaneous conjugates (Fig. 1D), but it is not clear if in the absence of cognate peptide the TCR engages in low affinity interactions with self-peptide/MHC complexes, or if MHC-II/CD4 interactions directly contribute to conjugate formation. The complete inhibition curves for Fig. 1D are presented in Fig. S2. Together, the above results show that the 3B11/LK35.2 cell pair efficiently forms conjugates and hence is suitable for AFM studies. However, this conjugate assay does not provide information on immune synapses and interaction forces, which were analyzed in the following set of experiments.

Immune Synapse Formation. T cells accumulate a multitude of their surface receptors, intracellular signaling and scaffolding molecules in the contact zone with APCs, resulting in the formation of a mature immune synapse. The IS is defined by a cluster of the TCR/CD3 complex in the center of the contact zone (central supramolecular activation cluster, cSMAC), which is surrounded by a second cluster containing LFA-1 (peripheral SMAC, pSMAC) (18). To study the kinetics of receptor accumulation and IS maturation at the contact zone of 3B11 T cells and LK35.2 B cells, all cell couples were analyzed by multispectral imaging flow cytometry (MIFC), using the Image Stream system. MIFC is a method that combines the advantages of a high-throughput flow cytometer and fluorescence microscopy (19), thereby allowing rapid quantitative and objective analysis of proteins in the contact zone between T cells and APCs for all T-cell/APC pairs within a given population.

Conjugates were stained for CD3 (cSMAC), LFA-1 (pSMAC), and F-actin (pSMAC) (20), and analyzed by MIFC. In the absence of HEL peptide, most T cells displayed a fairly equal distribution of CD3 and LFA-1 on the cell surface (Fig. 2A Upper Left), or randomized clusters of CD3 (see Fig. S3 for additional MIFC pictures). In contrast, in the presence of HEL peptide, strong polarization of both CD3 and LFA-1 in the contact zone was observed (Fig. 2A Upper Right). Quantification of T cells showing an enrichment of both CD3 and LFA-1 in the contact zone—and thus display a mature synapse—revealed that the peak number of mature immune synapses was reached after ≈30-min incubation time at 37 °C in the presence of HEL peptide (Fig. 2B). Thereafter, the number of T cells displaying a mature synapse started to decrease, but stayed above the level of values obtained without HEL peptide by at least a factor of 3. Interestingly, the amount of F-actin in the contact zone, which is crucial for the avidity regulation of integrins, increased over time (Fig. 2B). As a control, cells were preincubated with EDTA, which inhibits both integrin function and TCR/CD3-dependent calcium influx (16, 21). Hence, EDTA should abolish formation of a mature immune synapse. Fig. 2 shows that EDTA indeed inhibited both the maturation of the immune synapses and the accumulation of F-actin in the contact zone (Fig. 2B). Next, we analyzed whether the LFA-1 inhibitor, BIRT377, would affect the accumulation of LFA-1 and CD3 in the IS. Indeed, BIRT377 interfered with the accumulation of both LFA-1 and CD3 at the T-cell/B-cell interface and, concomitantly, disturbed mature IS formation (Fig. 2A Lower and C). Accumulation of F-actin in the contact zone was also strongly inhibited in the presence of BIRT377, demonstrating that activation of LFA-1 is required for both IS formation and stable accumulation of F-actin in the IS.

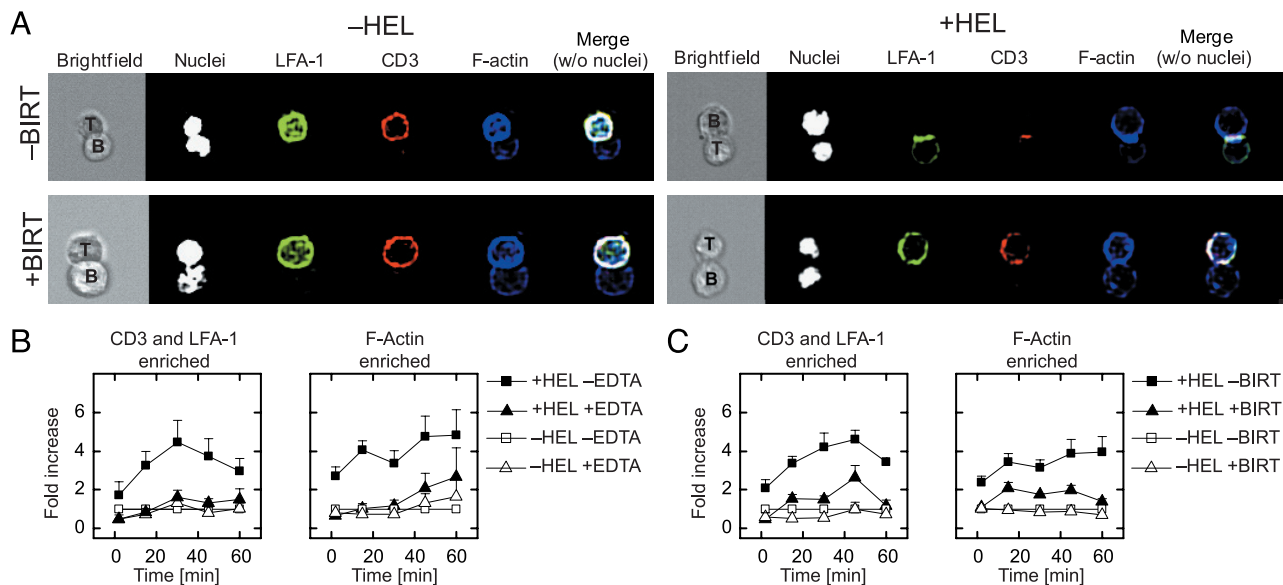


Fig. 2. Conjugates and synapse formation. (A) Representative MIFC pictures of T-cell/B-cell couples. Conjugates between 3B11 cells and unloaded (Left) or HEL_{34–45}-loaded (Right) LK35.2 cells were stained for LFA-1 (CD18-FITC, green), CD3 (red), or F-actin (Phalloidin, blue). Nuclei were stained with Hoechst (white); 20,000 events were acquired per sample. The pictures are representative of 3–4 independent experiments (mean, SE). Lower shows inhibition of synapse formation by BIRT377. Conjugates generated between 3B11 and LK35.2 cells with and without HEL_{34–45} peptide were inhibited by 80 μ M BIRT377. Additional MIFC pictures are presented in Fig. S3. (B) Kinetics of formation of mature immune synapses. Conjugates were generated in the presence or absence of EDTA and quantified by MIFC as described in A. Twenty thousand events were acquired for each sample. Percentages of T cells showing a mature immune synapse, i.e., an enrichment of both CD3 and LFA-1, were calculated as described in Materials and Methods. The graphic shows the mean \pm SE of 3–4 independent experiments. (C) The enrichment of CD3 plus LFA-1 and F-actin contact zone with BIRT377 is shown.

Interaction Forces Measured by AFM. The interaction forces between T cells and APC were measured in an AFM system equipped with a tissue-culture chamber for live cell experimentation. In orientating studies we determined that 3B11 T cells bound well to cantilevers coated with anti-CD43 antibodies, whereas the CD43-negative LK35.2 B cells adhere well to glass plates coated with polyL-lysine (PLL) without any signs of toxicity for the cells. AFM experiments were performed using custom-made Petri dishes divided into two chambers by a barrier. B cells were allowed to adhere to a PLL-coated glass plate placed into one chamber, whereas T cells were added to the other chamber. Using manual controls, the anti-CD43-coated cantilever was placed above a T cell whose viability had been confirmed by propidium iodide in the assay medium. The cantilever was advanced stepwise toward the T cell, and upon tapping the T cell adhered to the anti-CD43-coated cantilever without exerting high forces on the cell. The T cell was then hauled up, moved above a B cell (Fig. 3A), and lowered down for establishment of contact between the two cells. To allow for conjugate formation, we used forces in the range of 1–2 nN to press cells against each other, thereby ensuring that the T cell was in contact with the B cell. After various contact times, T_C , the cells were separated by retracting the cantilever over a range of $\approx 100 \mu\text{m}$. Laser deflection correlating to separation force curves during retraction was recorded and represents the interaction forces between cell conjugates.

Typical AFM force curves for $T_C = 30 \text{ min}$ are displayed in Fig. 3B. The curve designated (a) in Fig. 3B represents the interaction force curve obtained without HEL_{34–35} peptide, whereas (b) indicates the interaction force curve obtained with peptide. The line designated “Approach” indicates the approach of the cantilever with the B cell and establishment of contact. When the cantilever is retracted, it starts to bend until a certain point is reached after which molecular interactions begin to be disrupted. The total interaction force is defined as the differ-

ences of the lowest point of the spectrum and the value when the cantilever is fully retracted. In the examples shown in Fig. 3B, the interaction force for $T_C = 30 \text{ min}$ in the absence of antigen is 0.8 nN, and in the presence of antigen is 6.7 nN. Additional interaction force curves are shown in Fig. S4. Further hallmarks of AFM spectra can be seen in Fig. 3B. So-called *j-events* (22) are short force curve segments with a negative slope. They resemble jumps in the cantilever retraction and are usually correlated to breakages of single molecules or whole molecular clusters. They appear in the central section of spectra and have a short breakaway. In contrast, so-called *t-events* are discernible as step like structures at large Piezo positions when the cell bodies are already separated but still connected through viscous membrane nanotubes that carry one or several adhesion proteins on their tip. These nanotubes (also known as tethers) are viscously, that is, without force application, pulled out of the membrane reservoir.

A number of cell separation experiments failed because of technical difficulties. Failure rates increased especially at longer contact times (30 and 60 min). Although the cells were fixed to the cantilever or PLL-coated plate, respectively, the major part of the cells’ bodies were free to move, often resulting in separation or sliding into a parallel position so that the AFM cantilever would touch both cells. In AFM studies, investigators have often used the same cell attached to the cantilever for a large number of measurements (11, 23, 24). However, in these studies the contact times were usually short. Peptide-dependent interactions between T cells and APCs are probably special, because it has been shown that upon contact MHC-containing membrane fragments are pulled out from the APCs and remain bound to the T cell, a process termed trogocytosis that can operate in both directions (25). To avoid potential complications by such modified cells, we decided to select for each interaction force measurement a fresh pair of T cells and B cells. This

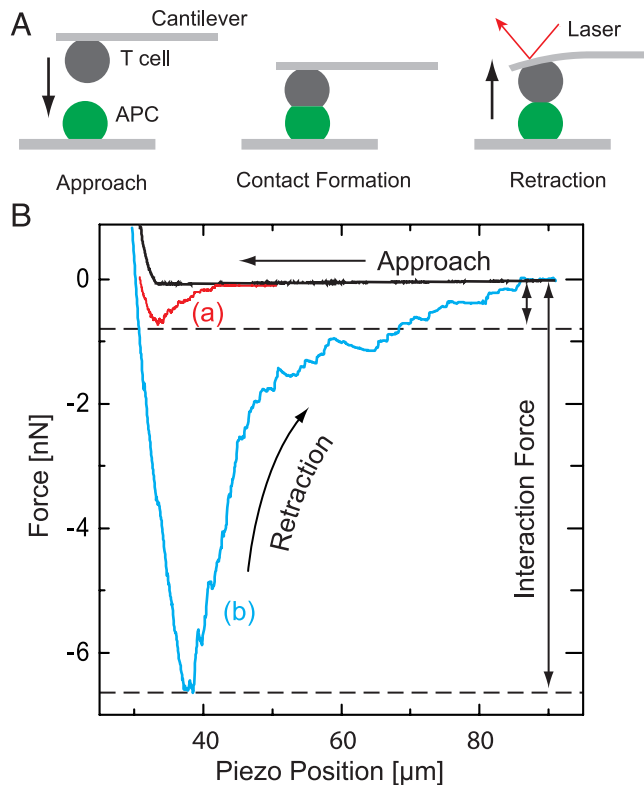


Fig. 3. Schematic illustration of AFM experiments. (A) A T cell is collected with an anti-CD43-coated cantilever and placed above a B cell that is attached to the PLL-coated bottom of a Petri dish. The T cell is then brought into contact with the B cell, and the T-cell/B-cell pair are left to form a conjugate without additional external force. After contact times, the cantilever is retracted, and interaction forces are measured by deflection of a laser beam. (B) AFM interaction force curves at $T_C = 30$ min. The curve labeled (a) shows the interaction curve obtained at $T_C = 30$ min without HEL₃₄₋₄₅ peptide, and (b) indicates the interaction force measures at $T_C = 30$ min in the presence of peptide. For a detailed description, see *Results*.

tedious and time-consuming procedure limited very much the number of measurements that could be performed.

In Fig. 4, the interaction force dynamics of 3B11/LK35.2 cell conjugates in the presence and absence of HEL peptide is shown. Fig. 4 includes a total of 92 successful measurements. At $T_C = 0$ min, cells were pressed against each other until the setpoint was reached and separated immediately afterward, resulting in a contact time of ≈ 1 –3 s. Interaction forces for all zero min time points yielded similar values for peptide pulsed and unpulsed cell pairs, namely 1.02 ± 0.46 nN and 1.08 ± 0.83 nN. Binding values remained similar after 2 min of contact. After $T_C = 15$ min, both pulsed and control pairs showed higher separation forces at 4.38 ± 3.37 nN and 2.48 ± 1.71 nN, respectively. At $T_C = 30$ min, the interaction force reached a maximum of 14.31 ± 3.64 nN for pulsed pairs, which represents a >10-fold increase compared with 1.28 ± 0.90 nN for control pairs. After 60 min contact time, pulsed values dropped back to 5.36 ± 4.25 nN and unpulsed to 0.95 ± 0.54 nN, demonstrating a decrease in the interaction forces after prolonged contact time. In five experiments with pulsed B cells, we observed forces >20 nN. However, we could not calculate the precise values because the T cell detached from the cantilever during separation due to the high forces. These experiments are not included in Fig. 4.

Our results, presented in Figs. 1 and 3, show that the LFA-1 antagonist BIRT377 interfered with maturation of the immune synapse and conjugate formation. Therefore, we decided to test the effect of BIRT377 on the interaction forces. Fig. 5 shows that

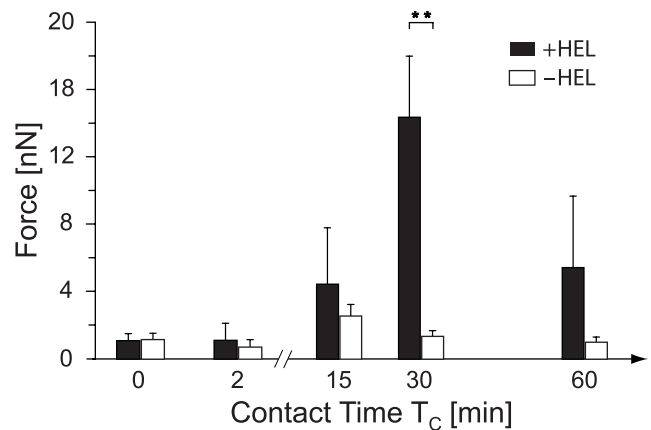


Fig. 4. Interaction force dynamics of 3B11/LK35.2 conjugates. LK35.2 cells pulsed with HEL₃₄₋₄₅ peptide (black bars) or without (white bars) were allowed to contact 3B11 T cells for the indicated time period, T_C . AFM force curves were subsequently recorded. In the presence of HEL₃₄₋₄₅ interaction, force values increase after $T_C = 15$ min, reach a maximum after 30 min, and decrease after 60 min, whereas values remain low in the absence of HEL₃₄₋₄₅. All bars, between 4 and 21 measurements. **, $P = 0.003$.

in the presence of BIRT the peptide-dependent interaction force value decreased from 14.3 nN to 0.4 nN. In the absence of peptides, the interaction force was also inhibited and dropped from 1.3 nN to 0.3 nN. These results establish the LFA-1/ICAM-1 pair of adhesion molecules as a critical component in the development of strong adhesion forces between T cells and APC. Because the force of interaction will be influenced by the number of ICAM-1 and LFA-1 molecules on the cell surface, it should be noted that the respective expression levels on the LK35.2 B cells and 3B11 T cells used here are within the normal range and comparable to primary activated B and T cells, to a number of B cell lines and T hybridomas tested (data not shown).

Discussion

In the past, AFM has been used to characterize interaction forces and kinetics in molecule-molecule binding. To that end, AFM cantilevers covered with immobilized ligands were contacted

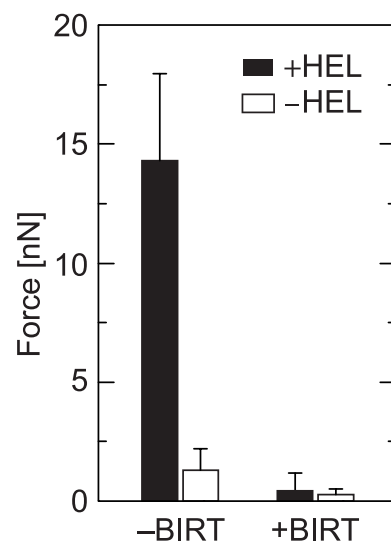


Fig. 5. Inhibition of conjugate adhesion strength by LFA-1 inhibitor. AFM interaction force measurements between LK35.2 and 3B11 cells were performed in the presence of $80 \mu\text{M}$ of LFA-1 inhibitor BIRT377. Interaction forces obtained in the presence and absence of HEL₃₄₋₄₅ are strongly reduced.

with receptor-coated surfaces and unbinding forces measured during the retraction phase. For antibody-antigen binding an interaction force of 244 ± 22 pN was reported (26), which is comparable in strength to the well studied strong streptavidin-biotin bond with an interaction force of 257 ± 25 pN (27). For investigation of membrane bound adhesion molecules in their native environment, cell-substrate studies have been conducted with various cell-ligand pairs. Moy and coworkers probed immobilized 3A9 (24) and Jurkat T cells (28) against ICAM-1-coated surfaces. Because the focus in those studies was the assessment of the bond strength of individual LFA-1/ICAM-1 complexes rather than overall forces on the cellular level, the cells were allowed to touch the substrates only for a few seconds, which is assumed to result in the formation of only one single binding. Benoit and coworkers pioneered the field of AFM based cell-cell adhesion measurements with *Dictyostelium discoideum* cells and found force values in the low nN regime for short contact times (11). In another study, Moy and coworkers examined interaction forces between human umbilical vein endothelial cells (HUVECs) and Jurkat T cells over a period of 10 s, yielding values in the range of 100 pN (13). Thus, so far, the majority of adhesion-related SCFS studies performed by AFM concentrated on short-time effects.

T cells need to switch effectively between different modes of adhesion. For example, adhesion properties change when T cells circulating in the blood stream start to migrate across the endothelial walls of blood vessels for infiltration into tissues. Likewise, for T-cell activation, intensive interactions with APCs are required. Because many of these adhesion events depend on integrins, T cells must tightly control their integrin activity. Hence, binding properties that build up over time have to be considered in cell-cell adhesion assays. It has been discussed that AFM may not be an appropriate tool for the investigation of long-term adhesion, because cells are motile and drifts may prevent experimental stability (12). However, despite these difficulties we have successfully measured the long-term dynamics of interaction forces in T-cell/APC conjugates with AFM-based SCFS in the present study. The number of successful measurements was limited by a substantial failure rate, particularly in the long-term measurements, despite the fact that cloned cell lines were used, which can be considered to be fairly homogenous. It is not clear whether these failures were due to high motility of the cells or other technical problems, or whether even cloned T cells and APCs may differ in their ability to form tight conjugates and immune synapses, for example depending on their cell cycle status. In preliminary AFM experiments with another T-cell hybridoma, we observed at $T_c = 30$ min an average interaction force of ≈ 12 nN in the presence of antigen (data not shown), which is comparable with the 14.3 nN found for the Lk35.2/3B11 pair. However, more cell pairs need to be tested for determination of the range of interaction forces.

A notable result of the present SCFS study is the observation that in the presence of peptide the interaction forces between T cells and APCs increase with time and reach a maximum after ≈ 30 min, whereas in the absence of peptide the binding forces remain low. This increase correlated well with the kinetics of IS formation, which also reached a maximum after ≈ 30 min, in agreement with other studies on IS formation (29). This relationship suggests that the strength of interaction forces depends on the state of IS maturity. Our observation that the small molecule inhibitor BIRT3777 inhibits both, the increase of interaction forces and IS formation, by blocking the activation of LFA-1, identifies LFA-1 as the major adhesion-inducing component in the IS investigated here. Moreover, this finding demonstrates that the interaction between TCR and pMHC is not responsible for the high interaction forces. Rather, our results indicate that after activation of TCR by pMHC T cells effectively switch between adhesion modes, whereby LFA-1

activation is triggered by an inside-out mechanism. This finding is in agreement with current views and shows how cells can control their adhesion propensity from the inside. Whether the spatial organization of LFA-1 within the contact zone influences the adhesion force, or vice versa, is not known at present.

It is interesting to note that in the FACS conjugate assay (see Fig. 1 B and C) a maximum of conjugate formation was already observed after a few minutes. This finding is in contrast to the more informative MIFC and AFM studies, which reveal that maximal synapse formation and interaction forces require ≈ 30 min for full development. Together, these observations suggest that weak interaction forces are sufficient to form conjugates (which are then stabilized by fixation with paraformaldehyde). Conjugates that formed in the absence of cognate peptide (Fig. 1 B and C) were inhibitable by BIRT377 and displayed low interaction forces (Fig. 5). These weak interactions resemble the transient interactions between T cells and DC observed in vivo in the absence of antigen, whereas the strong interaction forces with antigen correlate with the long-term interactions found in vivo in the presence of antigen (1).

Long-lasting interactions between T and B cells, which were investigated here, have also been demonstrated in vivo. The interaction force between T and B cells must be of considerable strength as it allows the cells to form stable pairs while migrating in the lymphatic environment, which is densely packed with other cells (19). Stable cell pairs are frequently encountered during the antigen-driven interactions of T cells with B cells in the area between B cell follicles and T-cell zones of lymph nodes in the early phase of immune responses (3) and during the germinal center response, where follicular helper T cells form tight conjugates with germinal center B cells (30). A failure of T cells to engage B cells in long-lasting interactions within lymph nodes results in severe defects of humoral immunity and is the cell-biological basis of X-linked lymphoproliferative disease (31).

In conclusion, the present study provides precise biophysical values for the interaction forces between T cells and APCs, and correlates the kinetics of synapse formation with the development of interaction forces. Although full synapse formation does not always seem to be required for activation of T cells (32), it is likely that strong interaction forces will favor optimal T-cell activation. The approach described here will allow further studies on the interrelationship between molecules influencing interaction forces, synapse formation, and T-cell activation.

Materials and Methods

Antigen Presentation and Cell Conjugate Assays. The murine T-cell hybridoma 3B11, recognizing the HEL₃₄₋₄₅ peptide (15), and the B cell lymphoma LK35.2 were maintained in RPMI MEDIUM 1640 tissue culture medium. For antigen presentation assays (33), 5×10^4 LK35.2 cells were pulsed with peptide for 4 h and incubated with 5×10^4 3B11 cells in triplicate in 96-well plates. After 40 h, IL-2 released by 3B11 cells was measured by an Europium-based fluorescence immunoassay. Cell conjugate assays were performed as reported (16). Briefly, 3B11 T cells were stained for 10 min at 37 °C with 0.5 μ mol of CFSE (Molecular Probes). LK35.2 cells were loaded with 100 μ mol of HEL₃₄₋₄₅ and labeled with 5 μ mol of SNARF (Invitrogen). Cells of each population (10^5) were mixed in 100 μ L medium, briefly centrifuged, fixed after various times with 2% paraformaldehyde, and analyzed with a FACS Calibur. BIRT377 was kindly provided by Terence Kelly (Boehringer Ingelheim).

Analysis of Immune Synapses by ImageStream (MIFC). For analysis of IS, conjugates were formed between 3B11 T cells and HEL peptide-loaded LK35.2 cells as described in ref. 20. Briefly, 1×10^6 cells were centrifuged in 250 μ L medium for formation of contacts and immediately resuspended in 50 μ L medium. After incubation at 37 °C for various time points, cells were fixed with 2% paraformaldehyde and stained with anti-CD3-biotin plus streptavidin TexasRed, anti-CD18-FITC (BD BioSciences), and nuclear dye (Hoechst-33342; Invitrogen) as indicated. Data acquisition (20,000 cells per sample) was performed with an ImageStream system (Amnis), and data were analyzed with IDEAS 3.0 software. To find the contact zone between 3B11 and LK35.2 cells, total events were gated on true T-cell/B-cell pairs and a Hoechst dye

dependent valley mask was defined between these coupled cells. The valley mask was combined with a T-cell mask that utilizes the CD3 staining. This results in the IS mask. Thereafter, protein accumulation was calculated as the ratio between the mean pixel intensity (MPI) of the respective protein, that is, CD3 or CD18, in the IS mask and the MPI of the same protein in the T cells mask.

AFM Measurements. The AFM system contained a "Nano-Wizard I" AFM with a CellHesion module (JPK Instruments AG) mounted on a AxioVert 200 microscope (Carl Zeiss). The AFM was placed in a CO₂ incubator box controlled by EMBL GPI68 IV system. Using a MatLab program, force curves were corrected for cantilever drift and different support positions. Data were analyzed with MATLAB (MathWorks). Silicon nitride tipless cantilevers (NSC 12 NoAl,

μmasch). Cantilever force constants ranged from 0.05–0.50 N/m as determined by individual calibration of the cantilever using the thermal noise method (34). For capture of T cells, cantilevers were coated with rat anti-mouse CD43 antibody (BD Biosciences) (Fig. S5). For AFM studies, modified Petri dishes were used as described in Fig. S5. Separation experiments were performed at constant retraction velocity of 1 $\mu\text{m/s}$ to ensure comparable conditions.

ACKNOWLEDGMENTS. We thank Daniel Aydin and Tobias Haas for discussions, and Susanne Bonifatius for expert technical support. This work was funded by the 6th Research Framework Program of the European Union, Project MUGEN LSHG-CT-2005-005203 (to G.J.H.), by the German Research Foundation, DFG SA393/3-3 (to Y.S.), and DFG SFB 405 (to G.J.H. and Y.S.).

1. Cahalan MD, Parker I (2005) Close encounters of the first and second kind: T-DC and T-B interactions in the lymph node. *Semin Immunol* 17:442–451.
2. von Andrian UH, Mempel TR (2003) Homing and cellular traffic in lymph nodes. *Nat Rev Immunol* 3:867–878.
3. Okada T, et al. (2005) Antigen-engaged B cells undergo chemotaxis toward the T zone and form motile conjugates with helper T cells. *PLoS Biol* 3:e150.
4. Delon J, Germain RN (2000) Information transfer at the immunological synapse. *Curr Biol* 10:R923–933.
5. Samstag Y, Eibert SM, Klemke M, Wabnitz GH (2003) Actin cytoskeletal dynamics in T lymphocyte activation and migration. *J Leukoc Biol* 73:30–48.
6. Luo BH, Springer TA (2006) Integrin structures and conformational signaling. *Curr Opin Cell Biol* 18:579–586.
7. Alon R, Dustin ML (2007) Force as a facilitator of integrin conformational changes during leukocyte arrest on blood vessels and antigen-presenting cells. *Immunity* 26:17–27.
8. Kinashi T (2005) Intracellular signaling controlling integrin activation in lymphocytes. *Nat Rev Immunol* 5:546–559.
9. Martinez-Rico C, et al. (2005) Separation force measurements reveal different types of modulation of E-cadherin-based adhesion by nectin-1 and -3. *J Biol Chem* 280:4753–4760.
10. Sung KL, et al. (1993) Determination of adhesion force between single cell pairs generated by activated GpIb-IIIa receptors. *Blood* 81:419–423.
11. Benoit M, Gabriel D, Gerisch G, Gaub HE (2000) Discrete interactions in cell adhesion measured by single-molecule force spectroscopy. *Nat Cell Biol* 2:313–317.
12. Benoit M, Gaub HE (2002) Measuring cell adhesion forces with the atomic force microscope at the molecular level. *Cells Tissues Organs* 172:174–189.
13. Zhang X, Wojcikiewicz EP, Moy VT (2006) Dynamic adhesion of T lymphocytes to endothelial cells revealed by atomic force microscopy. *Exp Biol Med* 231:1306–1312.
14. Muller DJ, Dufrene YF (2008) Atomic force microscopy as a multifunctional molecular toolbox in nanobiotechnology. *Nat Nano* 3:261–269.
15. Momburg F, et al. (1993) Epitope-specific enhancement of antigen presentation by invariant chain. *J Exp Med* 178:1453–1458.
16. Gunzer M, et al. (2004) A spectrum of biophysical interaction modes between T cells and different antigen-presenting cells during priming in 3-D collagen and in vivo. *Blood* 104:2801–2809.
17. Kelly TA, et al. (1999) Cutting edge: A small molecule antagonist of LFA-1-mediated cell adhesion. *J Immunol* 163:5173–5177.
18. Monks CR, Freiberg BA, Kupfer H, Sciaky N, Kupfer A (1998) Three-dimensional segregation of supramolecular activation clusters in T cells. *Nature* 395:82–86.
19. McGrath KE, Bushnell TP, Palis J (2008) Multispectral imaging of hematopoietic cells: Where flow meets morphology. *J Immunol Methods* 336:91–97.
20. Reichardt P, et al. (2007) Naive B cells generate regulatory T cells in the presence of a mature immunologic synapse. *Blood* 110:1519–1529.
21. Donnadieu E, Bismuth G, Trautmann A (1992) Calcium fluxes in T lymphocytes. *J Biol Chem* 267:25864–25872.
22. Helenius J, Heisenberg C-P, Gaub HE, Muller DJ (2008) Single-cell force spectroscopy. *J Cell Sci* 121:1785–1791.
23. Schmitz J, Benoit M, Gottschalk KE (2008) The viscoelasticity of membrane tethers and its importance for cell adhesion. *Biophys J* 95:1448–1459.
24. Zhang X, Wojcikiewicz E, Moy VT (2002) Force spectroscopy of the leukocyte function-associated antigen-1/intercellular adhesion molecule-1 interaction. *Biophys J* 83:2270–2279.
25. Hudrisier D, Aucher A, Puaux AL, Bordier C, Joly E (2007) Capture of target cell membrane components via trogocytosis is triggered by a selected set of surface molecules on T or B cells. *J Immunol* 178:3637–3647.
26. Hinterdorfer P, Baumgartner W, Gruber HJ, Schilcher K, Schindler H (1996) Detection and localization of individual antibody-antigen recognition events by atomic force microscopy. *Proc Natl Acad Sci USA* 93:3477–3481.
27. Moy VT, Florin EL, Gaub HE (1994) Intermolecular forces and energies between ligands and receptors. *Science* 266:257–259.
28. Wojcikiewicz EP, Abdulreda MH, Zhang X, Moy VT (2006) Force spectroscopy of LFA-1 and its ligands, ICAM-1 and ICAM-2. *Biomacromolecules* 7:3188–3195.
29. Grakoui A, et al. (1999) The immunological synapse: A molecular machine controlling T cell activation. *Science* 285:221–227.
30. Allen CD, Okada T, Tang HL, Cyster JG (2007) Imaging of germinal center selection events during affinity maturation. *Science* 315:528–531.
31. Qi H, Cannons JL, Klauschen F, Schwartzberg PL, Germain RN (2008) SAP-controlled T-B cell interactions underlie germinal centre formation. *Nature* 455:764–769.
32. Brossard C, et al. (2005) Multifocal structure of the T cell–dendritic cell synapse. *Eur J Immunol* 35:1741–1753.
33. Brocke P, Armandola E, Garbi N, Hammerling GJ (2003) Downmodulation of antigen presentation by H2-O in B cell lines and primary B lymphocytes. *Eur J Immunol* 33:411–421.
34. Cleveland JP, Manne S, Bocek D, Hansma PK (1993) A nondestructive method for determining the spring constant of cantilevers for scanning force microscopy. *Rev Sci Instrum* 64:403–405.